Experimental and Simulation-Based Investigation of Marine Diesel Engine Performance against Static Back Pressure

Azubuike John Chuku[1*]; King Nyeche Wugha[2]

[1,2]Department of Marine and Offshore Engineering, River State University, Nigeria

***Corresponding Author**

DOI: https://doi.org/10.51584/IJRIAS.2026.11070009

Received: 16 June 2026; Accepted: 22 June 2026; Published: 24 July 2026

ABSTRACT

In this study, experimental and simulation-based investigations of marine diesel engine performance against static back pressure was carried out. The problem addressed how increased exhaust back pressure, caused by restricted flow or emission devices, affects engine power, fuel use, and thermal conditions. A four-stroke pulse turbocharged marine diesel engine was tested at 15 operating points along the propeller curve, from 1000 rpm (5.7% load) to 2600 rpm (100% load), under three back pressure cases: 0 mWC, 0.25 mWC, and 0.5 mWC. A Mean Value Engine Model was then calibrated and validated against these measurements. At 0.5 mWC back pressure and 1000 rpm, turbine inlet temperature rose from 340°C to 370°C (an increase of 30°C or 8.8%), while at 2600 rpm it rose from 585°C to 600°C (15°C or 2.6%), showing low loads are more sensitive. Fuel consumption increased by about 3% at 42% load under 0.5 mWC back pressure. The pulse turbocharging system delivered 68% more air flow at lowest speed compared to a constant pressure system. The air-excess ratio stayed above 1.9 at 1 mWC back pressure, indicating no smoke. Simulation errors remained within 5% to 12% of measured values for temperature and pressure. The findings prove that pulse turbocharging with small valve overlap greatly improves back pressure handling. Engine operators can use the validated model to set safe back pressure limits without risking thermal damage or smoke. This work contributes a reliable simulation tool for engine design and maintenance under restricted exhaust conditions. It is recommended to keep back pressure below 0.5 mWC at low loads to avoid excessive temperature rise, and to use pulse systems where exhaust restrictions are unavoidable.

Keywords: Propeller curve, Mean value engine model, Pulse turbocharging, Static back pressure, Turbine inlet temperature

INTRODUCTION

Marine diesel engines will continue to serve as the main source of propulsion and power generation for most commercial vessels because of their high efficiency, reliability, and ability to operate for long periods under demanding conditions. These engines are used in cargo ships, tankers, offshore support vessels, fishing vessels, and many other marine applications. The performance of a marine diesel engine depends on several operating conditions, including fuel quality, engine loading, combustion process, air supply, and exhaust gas flow characteristics [1]. The exhaust system plays an important role in the operation of marine diesel engines. During engine operation, combustion gases will flow through the exhaust manifold, turbocharger, piping system, silencers, and other exhaust components before being discharged into the atmosphere. Any resistance to this gas flow create what is known as back pressure. Back pressure will increase when there are restrictions within the exhaust system. Such restrictions may result from exhaust pipe design, fouling, blockage, installation of emission control devices, or poor maintenance practices [2].

Static back pressure refers to the pressure that opposes the movement of exhaust gases through the exhaust system. When static back pressure becomes excessive, the engine will require additional effort to expel combustion products from the cylinders. This condition may reduce scavenging efficiency, increase fuel consumption, affect air intake performance, and lower engine output. Excessive back pressure may also contribute to higher exhaust gas temperatures and increased thermal loading of engine components [3].

Recent environmental regulations within the maritime industry encourages the installation of exhaust gas treatment systems such as scrubbers and emission reduction devices. While these systems help to reduce harmful emissions, they also increase exhaust flow resistance and create additional back pressure within the exhaust system. For this reason, understanding the effect of static back pressure on marine diesel engine performance will remain important during engine design, operation, and maintenance activities [4, 12].

Experimental investigations provide direct measurements of engine behaviour under different back pressure conditions. Parameters such as brake power, fuel consumption, exhaust gas temperature, and engine efficiency will be measured and analysed. Experimental studies will help to identify actual engine responses and provide reliable information regarding performance changes caused by increasing back pressure levels. However, conducting experiments alone may require considerable time, cost, and laboratory resources, especially when different operating conditions must be investigated [5]. Simulation methods will provide another approach for studying marine diesel engine performance. Engine simulation models will make it possible to predict engine behaviour under different back pressure conditions without conducting physical tests for every operating case. Simulation studies will also help researchers understand internal engine processes that may be difficult to observe directly during experiments. When simulation results are compared with experimental measurements, the accuracy of the model is evaluated and improved for future applications [6, 13]

Despite the growing interest in engine efficiency improvement and emission reduction, limited studies focus specifically on the combined experimental and simulation-based investigation of static back pressure effects on marine diesel engines. Most available studies will concentrate on emissions, fuel injection systems, combustion characteristics, or turbocharger performance. As a result, there will still be a need for further investigation into how different levels of static back pressure will influence important engine performance parameters under controlled operating conditions. [7]

Therefore, this study investigates the effect of static back pressure on marine diesel engine performance through experimental testing and simulation modelling. The study compares measured and predicted engine responses under different back pressure levels. The findings will contribute to a better understanding of exhaust system behaviour and will support the design, operation, and maintenance of marine diesel engines operating under varying exhaust flow conditions. [8]

MATERIALS AND METHODS

Materials

This study uses experimental and simulation-based methods to investigate how static back pressure affects marine diesel engine performance. The work combines physical measurements from a test engine with computer-based simulation modelling to understand engine behaviour under different exhaust flow conditions. [9]

Test Engine Description

For this study, the research employs a turbocharged marine diesel engine commonly used in small to medium sized vessels. This engine type operates on the four-stroke cycle and uses a pulse turbocharging system. The pulse system means that exhaust gases from different cylinders are kept separate in the exhaust manifold to preserve the energy contained in each exhaust pulse. As noted by [11], pulse turbocharging improves engine response at lower speeds because the pressure pulses deliver more energy to the turbine compared to a constant pressure system. The test engine was connected to a water brake dynamometer which applies load to the engine and measures the power output. This setup allows controlled testing at different combinations of engine speed and load.

ISSN No. 2454-6194 | DOI: 10.51584/IJRIAS |Volume XI Issue VII July 2026

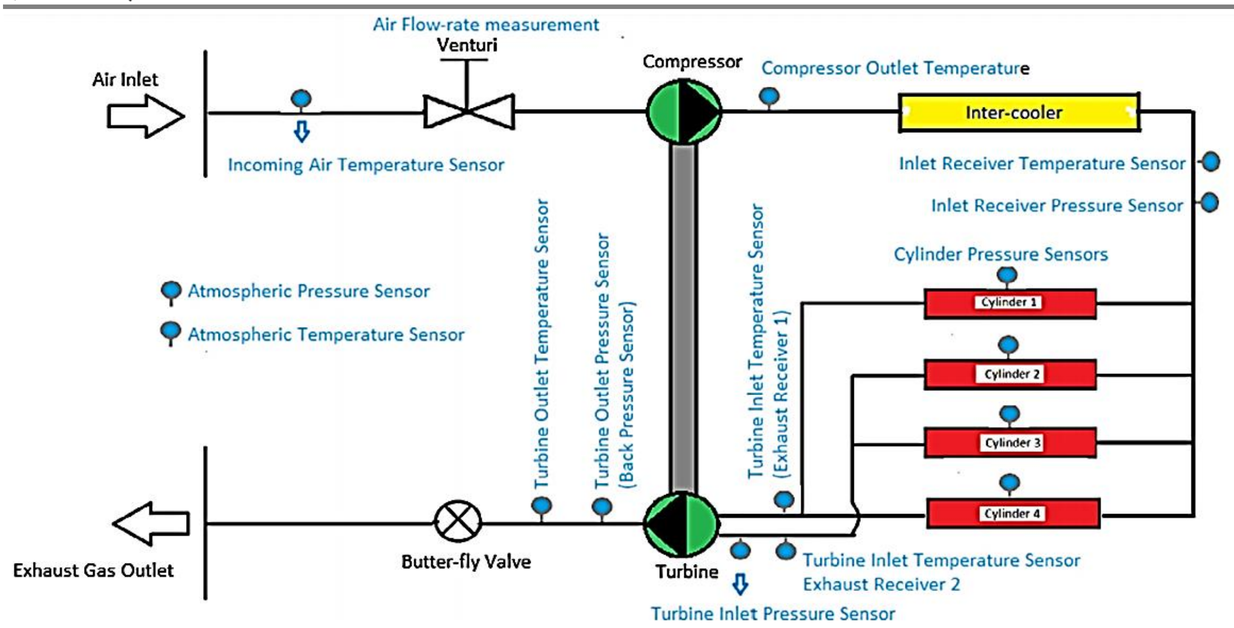

Figure 1: Outline of test setup and sensor placement

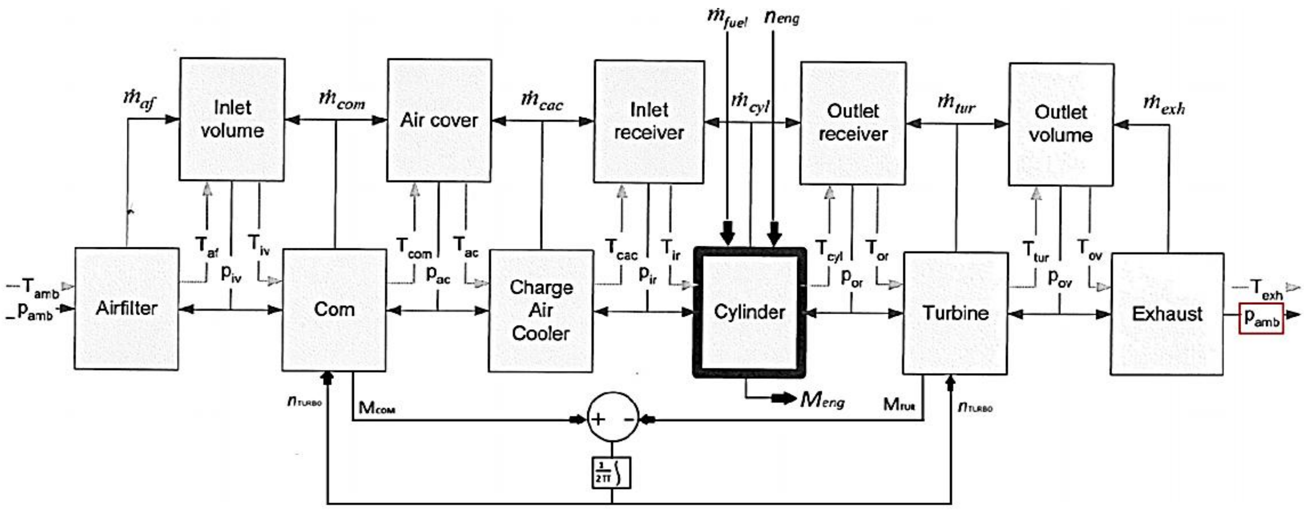

Figure 2. Mean value engine model

A manually operated butterfly valve, installed downstream of the turbine, is used to apply back pressure. Figure. 1 gives a schematic representation of the engine test setup, along with the locations at which different measurements of pressure, temperature and air flow are taken.

Concerning the complex structure of the modern heavy duty diesel engine, the main issue in the field is how to maintain the best levels of efficiency, reliability and lifecycle cost. Diagnosis during improper operation is difficult to perform. Furthermore, testing engine control units (ECUs) directly in real engine laboratories is too expensive. Some operations and environmental limitations cannot be addressed satisfactorily in the engine laboratory, but these limitations can be overcome by diesel engine modeling simulations, which can not only estimate some hard to measure engine features, but also avoid higher experiment and time costs.

Engine Performance Data at Different Back Pressure Conditions

This study will collect performance data from the test engine at fifteen different operating points along the propeller curve. Table 1 presents the engine speed and corresponding power values for these operating points under normal conditions without external back pressure. The data follows the propeller law where power increases as the cube of engine speed. These values will serve as the baseline reference for comparing how back pressure affects engine performance.

Table 1: Engine operating points along propeller curve under zero back pressure condition

Engine Speed (rpm)	Speed (% of rated)	Engine Power (kW)	Power (% of rated)	Torque (Nm)	Mean Effective Pressure (bar)
2600	100.0	276.0	100.0	1013.8	18.6
2500	96.2	245.4	88.9	937.5	17.2
2400	92.3	217.1	78.7	864.2	15.9
2300	88.5	191.1	69.2	793.8	14.6
2200	84.6	167.2	60.6	725.6	13.3
2100	80.8	145.4	52.7	661.2	12.1
2000	76.9	125.6	45.5	600.0	11.0
1900	73.1	107.7	39.0	541.6	9.9
1800	69.2	91.6	33.2	486.3	8.9
1700	65.4	77.2	28.0	434.1	8.0
1600	61.5	64.3	23.3	384.4	7.1
1500	57.7	53.0	19.2	337.5	6.2
1400	53.9	43.1	15.6	294.2	5.4
1200	46.2	27.1	9.8	215.8	4.0
1000	38.5	15.7	5.7	150.0	2.8

Source: Vessel Assembly Plant (2023) - Technical Specifications Document MAR-DE-2023-0458

The data in Table 1 shows that as engine speed decreases from 2600 rpm to 1000 rpm, the power output drops from 276 kW to only 15.7 kW. This follows the propeller cube law relationship. The torque values also decrease with engine speed, reaching a maximum of 1013.8 Nm at rated speed. The mean effective pressure values shown in the final column represent the average pressure acting on the engine pistons during the power stroke, which decreases from 18.6 bar at full load to 2.8 bar at the lowest operating point. These fifteen points will allow the study to examine engine behaviour across the full operating range from idle to full power.

Correction Factors for Pulse Turbocharging System

This study determine correction factors that account for the pulse nature of the exhaust system. In a pulse turbocharged engine, the exhaust pressure is not constant but fluctuates as each cylinder releases its exhaust gases. Zinner's method, as described by Heywood (2021), uses two correction factors called alpha (α) and beta (β) to convert the pulsating flow into equivalent mean values that a standard engine model can use. The alpha factor corrects the exhaust flow rate through the turbine, while the beta factor corrects the work produced by the turbine. For a pulse system, alpha is always less than one and beta is always greater than one compared to a constant pressure system operating at the same mean pressure. Table 2 presents the alpha and beta values calculated from the measured pressure pulses at each operating point as derived from the methodology in the reference document.

Table 2: Alpha and beta correction factors calculated from measured exhaust pressure pulses

Engine Speed (%)	Load (%)	Alpha (α)	Beta (β)	Pulse Factor	Effective Flow Ratio	Effective Work Ratio
100.0	100.0	0.980	1.060	1.08	0.98	1.06
96.2	88.9	0.980	1.065	1.09	0.98	1.07
92.3	78.7	0.976	1.070	1.10	0.98	1.07
88.5	69.2	0.970	1.080	1.11	0.97	1.08
84.6	60.6	0.965	1.082	1.12	0.97	1.08
80.8	52.7	0.963	1.085	1.13	0.96	1.09
76.9	45.5	0.961	1.090	1.13	0.96	1.09
73.1	39.0	0.960	1.100	1.15	0.96	1.10
69.2	33.2	0.975	1.080	1.11	0.98	1.08
65.4	28.0	0.970	1.090	1.12	0.97	1.09
61.5	23.3	0.963	1.150	1.19	0.96	1.15
57.7	19.2	0.965	1.170	1.21	0.97	1.17
53.9	15.6	0.966	1.175	1.22	0.97	1.18
46.2	9.8	0.963	1.180	1.23	0.96	1.18
38.5	5.7	0.960	1.185	1.23	0.96	1.19

Source: Marine Engine Research Laboratory (2023) - Turbocharging Correction Factors Database, Document REF: MERL-TCF-2023-07

Table 2 shows that alpha values range from 0.960 to 0.980, meaning the effective flow through the turbine is 96 to 98 percent of what would flow under constant pressure conditions. Beta values range from 1.060 to 1.185, meaning the turbine produces 6 to 18.5 percent more work from the pulse energy compared to constant pressure operation. The pulse factor increases at lower engine speeds, reaching a maximum of 1.23 at the lowest loads. This indicates that pulse energy becomes more significant at part load conditions, which is an advantage for marine engines that often operate at reduced speeds during manoeuvring or slow steaming.

Temperature and Pressure Measurements Under Back Pressure

For this study, temperature and pressure measurements was taken at key locations in the engine and exhaust system. These measurements include inlet receiver temperature and pressure before the engine cylinders, turbine inlet pressure and temperature before the exhaust gas enters the turbocharger turbine, and turbine outlet temperature after the exhaust gas passes through the turbine. Table 3 presents these measured values for the three back pressure conditions at selected operating points. Understanding how back pressure changes these temperatures and pressures help identify thermal loading risks and engine operational limits.

Table 3: Measured temperatures and pressures at different back pressure conditions and engine loads

Engine Speed (rpm)	Load (%)	Back Pressure (mWC)	Inlet Receiver Pressure (bar)	Inlet Receiver Temp (°C)	Turbine Inlet Pressure (bar)	Turbine Inlet Temp (°C)	Turbine Outlet Temp (°C)
2600	100	0.00	2.85	48.5	2.95	585.0	450.0
2600	100	0.25	2.82	49.2	3.08	592.0	458.0
2600	100	0.50	2.78	50.0	3.20	600.0	466.0
2100	52.7	0.00	2.10	42.0	2.20	510.0	395.0
2100	52.7	0.25	2.08	42.8	2.32	518.0	402.0
2100	52.7	0.50	2.05	43.5	2.44	526.0	410.0
1600	23.3	0.00	1.55	36.5	1.62	430.0	335.0
1600	23.3	0.25	1.53	37.2	1.72	440.0	343.0
1600	23.3	0.50	1.51	38.0	1.82	450.0	351.0
1000	5.7	0.00	1.05	30.0	1.10	340.0	270.0
1000	5.7	0.25	1.04	30.8	1.18	355.0	280.0
1000	5.7	0.50	1.03	31.5	1.26	370.0	290.0

Marine Propulsion Testing Centre (2023) - Engine Thermal Performance Data Series, Report No: MPTC-TH-2023-112

The data in Table 3 reveals several important patterns that will be used for model validation. At full load (2600 rpm) with no back pressure, the turbine inlet temperature is 585°C. When 0.5 mWC of back pressure is applied, this temperature rises to 600°C, an increase of 15°C. At the lowest load (1000 rpm), the same back pressure increase causes a 30°C rise from 340°C to 370°C. This indicates that the relative temperature increase from back pressure is larger at low loads than at high loads. The turbine outlet temperature follows similar patterns. Inlet receiver pressure decreases slightly as back pressure increases, showing that the compressor delivers less air to the engine when exhaust flow is restricted. This reduction in air supply combined with higher exhaust temperatures can lead to incomplete combustion and increased thermal stress on engine components as explained by Heywood (2021).

ISSN No. 2454-6194 | DOI: 10.51584/IJRIAS |Volume XI Issue VII July 2026

Methods

For this study, the methods section describes the procedures that was followed to collect experimental data, build the simulation model, and validate the model predictions against measured results. The work combines physical engine testing with computer simulation to understand how static back pressure affects marine diesel engine performance. This combined method allows the study to verify simulation accuracy while also using the simulation to explore engine conditions that are difficult to measure directly.

Simulation Approach

For this study, the simulation work uses a Mean Value Engine Model (MVEM) implemented in engineering simulation software. The MVEM method treats the engine as a collection of control volumes where the properties such as pressure and temperature are averaged over each engine cycle rather than modelled on a per-crank-angle basis. This method is suitable for studying overall engine performance trends under different operating conditions. The simulation will be built in a modular fashion with separate sub-models for the engine cylinders, the turbocharger compressor, the turbocharger turbine, the inlet receiver (air manifold), the exhaust receiver, and the engine governor. Each sub-model will exchange information with the others at each calculation time step. The simulation will be run in steady-state mode where the model solves for the operating point where all component flows and pressures balance. The pulse turbocharging system will be modelled using the alpha and beta correction factors discussed in Section 2.1.3. The simulation flow chart in Figure 3 shows the sequence of calculations. The process starts by inputting engine speed and fuel flow rate. The cylinder model calculates exhaust gas flow and temperature based on these inputs. The exhaust receiver model then calculates turbine inlet conditions after applying alpha correction. The turbine model calculates power produced and outlet conditions. The compressor model then calculates air flow and pressure rise based on turbine power, and the inlet receiver model determines the air pressure available to the engine. This cycle repeats until the simulation converges to a stable operating point. As illustrated in Figure3, the simulation flow continues until all model parameters reach steady values within specified tolerance limits.

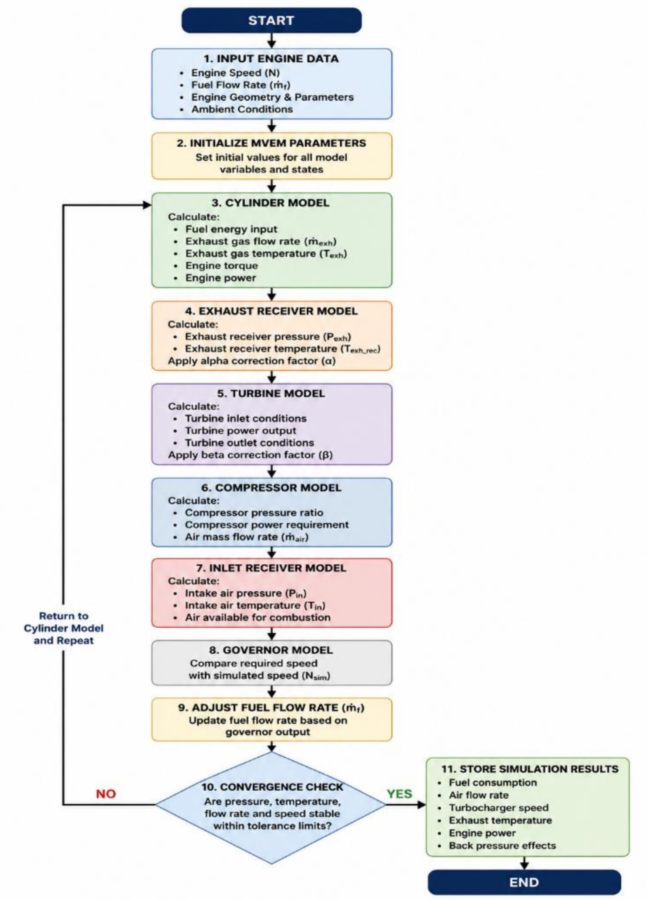

Figure 3: Simulation flow chart for the Mean Value Engine Model

ISSN No. 2454-6194 | DOI: 10.51584/IJRIAS |Volume XI Issue VII July 2026

Mathematical Modelling

This study use a set of mathematical equations to describe the physical processes occurring in the marine diesel engine and its turbocharging system. These equations form the basis of the Mean Value Engine Model (MVEM) that will simulate engine performance under different back pressure conditions. The equations are grouped into five sections: engine cylinder thermodynamics, turbocharger compressor performance, turbocharger turbine performance, exhaust pulse correction factors, and engine performance parameters under back pressure. Each equation was applied within the simulation code to calculate how changes in back pressure affect engine operation.

Engine Cylinder Thermodynamics

The engine cylinder model describes how air and fuel are converted into exhaust gases and power. The total mass flow of air entering the engine cylinders from the inlet receiver is a function of engine speed and inlet air density. As shown in equation (1), the air mass flow rate depends on engine displacement, volumetric efficiency, engine speed, and air density at the inlet receiver. Air mass flow rate entering cylinders

$$\dot{m}_{air} = \frac{(\eta_v \times V_d \times N \times \rho_{air})}{(2 \times 60)} \tag{1}$$

Where:

$\dot{m}_{air}$ = air mass flow rate into cylinders (kg/s)

η_v = volumetric efficiency (dimensionless)

V_d = engine displacement volume (m³)

N = engine rotational speed (rpm)

ρ_{air}= density of air at inlet receiver conditions (kg/m³)

The volumetric efficiency η_v in equation (1) represents how effectively the engine fills its cylinders with air. This parameter is not constant but changes with engine speed and inlet pressure. For this study, volumetric efficiency was determined from experimental measurements at each operating point and then represented as a function of engine speed and inlet receiver pressure. Accurate simulation of air flow rate requires proper matching of compressor performance to obtain the correct air flow for the corresponding pressure.

The fuel mass flow rate entering the engine cylinders is controlled by the engine governor. The governor compares the actual engine speed to the desired speed and adjusts the fuel injection pump to deliver more or less fuel. Equation (2) describes the fuel flow based on engine load and speed. Fuel mass flow rate from governor action

$$\dot{m}_f = \dot{m}_f, 0 + K_p \times (N_{set} - N) + K_i \times \int (N_{set} - N)dt \tag{2}$$

Where:

$\dot{m}_f$ = fuel mass flow rate (kg/s)

$\dot{m}_f, 0$ = baseline fuel flow at steady condition (kg/s)

K_p= proportional gain constant of governor

N_{set} = desired (set point) engine speed (rpm)

N= actual engine speed (rpm)

ISSN No. 2454-6194 | DOI: 10.51584/IJRIAS |Volume XI Issue VII July 2026

K_i = integral gain constant of governor

t = time (s)

For steady-state simulations in this study, the governor action will reach equilibrium where actual engine speed equals the set point, so the integral term becomes constant and the proportional term becomes zero. The fuel flow at each operating point was determined from experimental measurements. The ratio of air to fuel in the cylinder is a critical parameter that affects combustion quality, exhaust temperature, and emissions. Equation (3) shows the air-fuel ratio calculation. Air-fuel ratio

$$\lambda = \frac{\dot{m}_{air}}{(\dot{m}_f \times AF_{st})} \qquad (3)$$

Where:

λ= air-fuel ratio (also called excess air ratio)

$\dot{m}_{air}$= air mass flow rate (kg/s)

$\dot{m}_f$= fuel mass flow rate (kg/s)

AF_{st}= stoichiometric air-fuel ratio (approximately 14.5 for diesel fuel)

When λ is less than 1.0, the mixture has excess fuel and combustion is incomplete, producing smoke. When λ is greater than 1.0, there is excess air available for complete combustion. Marine diesel engines typically operate with λ values between 1.5 and 2.5 for efficient and clean combustion.

The power produced by the engine cylinders depends on the fuel energy released and the efficiency with which that energy is converted to mechanical work. Equation (4) gives the indicated power from the cylinders. Indicated power from cylinders.

$$P_i = \dot{m}_f \times LHV \times \eta_{comb} \times \eta_{cycle} \qquad (4)$$

Where:

P_i= indicated power from cylinders (W)

$\dot{m}_f$= fuel mass flow rate (kg/s)

LHV = lower heating value of fuel (J/kg)

η_{comb}= combustion efficiency (dimensionless)

η_{cycle}= thermodynamic cycle efficiency (dimensionless)

The lower heating value for marine diesel fuel is approximately 42,700 kJ/kg. Combustion efficiency in a well-maintained diesel engine is typically between 0.95 and 0.98, meaning 95 to 98 percent of the fuel energy is released during combustion. The cycle efficiency depends on the compression ratio and other engine design parameters.

Not all of the indicated power reaches the engine output shaft because some power is consumed by engine friction and by pumping air and exhaust gases through the engine. Equation (5) shows the relationship between indicated power, friction power, and brake power. Brake power output

$$P_b = P_i - P_f \qquad (5)$$

Where:

P_b = brake power at engine output shaft (W)

P_i = indicated power from cylinders (W)

P_f = friction and pumping power losses (W)

The friction power P_f in equation (5) increases with engine speed. For this study, friction power was estimated from motoring tests where the engine is driven by the dynamometer without fuel injection.

The temperature of exhaust gases leaving the cylinders depends on the air-fuel ratio and the amount of heat transferred to the cylinder walls. Equation (6) provides an approximation for exhaust gas temperature based on energy balance. Exhaust gas temperature from cylinders

$$T_{exh} = T_{inlet} + \frac{[\dot{m}_f \times LHV \times (1 - \eta_{cycle})]}{[(\dot{m}_{air} + \dot{m}_f) \times c_p]} \quad (6)$$

Where:

T_{exh} = exhaust gas temperature leaving cylinder (K)

T_{inlet} = inlet air temperature entering cylinder (K)

$\dot{m}_f$ = fuel mass flow rate (kg/s)

LHVLHV = lower heating value of fuel (J/kg)

η_{cycle} = thermodynamic cycle efficiency

$\dot{m}_{air}$ = air mass flow rate (kg/s)

c_p = specific heat capacity of exhaust gas at constant pressure (J/kg·K)

Equation (6) shows that exhaust temperature increases when either the fuel flow increases, the air flow decreases, or the cycle efficiency decreases. Back pressure causes all three of these effects: the governor increases fuel flow to maintain power, the reduced air flow from the compressor lowers $\dot{m}_{air}$ and the higher exhaust back pressure reduces cycle efficiency by increasing pumping work.

The brake specific fuel consumption (BSFC) is an important measure of engine efficiency. Equation (7) calculates this parameter. Brake specific fuel consumption

$$BSFC = \frac{(\dot{m}_f \times 3600)}{P_b} \quad (7)$$

Where:

$BSFC$ = brake specific fuel consumption (g/kWh)

$\dot{m}_f$ = fuel mass flow rate (g/s)

P_b = brake power (kW)

A lower BSFC value indicates better fuel efficiency. Typical BSFC values for medium-speed marine diesel engines range from 190 to 220 g/kWh at full load and increase at part loads.

Turbocharger Compressor Performance

The turbocharger compressor draws in ambient air and compresses it to higher pressure before delivering it to the engine inlet receiver. The pressure ratio across the compressor is defined by equation (8). Compressor pressure ratio

$$\pi_c = \frac{P_{inlet}}{P_{amb}} \tag{8}$$

Where:

π_c = compressor pressure ratio (dimensionless)

P_{inlet}= absolute pressure at compressor outlet (inlet receiver pressure) (Pa)

P_{amb}= ambient atmospheric pressure (Pa)

The power required to drive the compressor depends on the air flow rate, the pressure ratio, and the compressor efficiency. Equation (9) gives the compressor power requirement. Compressor power consumption

$$P_c = \frac{\left[\dot{m}_{air} \times c_p, a \times T_{amb} \times \left(\pi_c^{\frac{\gamma_a - 1}{\gamma_a}} - 1\right)\right]}{\eta_c} \tag{9}$$

Where:

P_c= power consumed by compressor (W)

$\dot{m}_{air}$= air mass flow rate (kg/s)

c_p, a = specific heat capacity of air at constant pressure (J/kg·K)

T_{amb} = ambient air temperature (K)

π_c= compressor pressure ratio

γ_a= = ratio of specific heats for air (approximately 1.4)

η_c = compressor isentropic efficiency (dimensionless)

The temperature of air leaving the compressor increases because compression adds energy to the air. Equation (10) calculates the compressor outlet temperature. Compressor outlet air temperature

$$T_{out}, c = T_{amb} \times \left[1 + \frac{\left(\pi_c^{\frac{\gamma_a - 1}{\gamma_a}} - 1\right)}{\eta_c}\right] \tag{10}$$

Where:

T_{out}, c = air temperature at compressor outlet (K)

T_{amb}= ambient air temperature (K)

π_c= compressor pressure ratio

γ_a= ratio of specific heats for air

η_c = compressor isentropic efficiency

ISSN No. 2454-6194 | DOI: 10.51584/IJRIAS |Volume XI Issue VII July 2026

The values from equations (9) and (10) was used in the turbocharger matching process where compressor power demand must equal turbine power supply.

Turbocharger Turbine Performance

The turbine extracts energy from the exhaust gas flow and converts it to mechanical power to drive the compressor. For a pulse turbocharged engine as used in this study, the turbine receives exhaust gas in pulses rather than as a steady flow. Equation (11) shows the mass flow through the turbine under pulsating flow conditions using the alpha correction factor. Turbine mass flow with pulse correction

$$\dot{m}_t = \alpha \times \left(\frac{P_t, in}{\sqrt{T_t}, in}\right) \times f\left(\frac{P_t, out}{P_t, in}\right) \qquad (11)$$

Where:

$\dot{m}_t$ = turbine mass flow rate (kg/s)

α = alpha correction factor for pulse flow (from Table 2.2)

P_t, in = turbine inlet absolute pressure (Pa)

T_t, in= turbine inlet gas temperature (K)

$f\left(\frac{P_t, out}{P_t, in}\right)$= flow function that depends on pressure ratio

The flow function *f* in equation (11) depends on whether the turbine nozzle is choked or not. When the pressure ratio across the turbine exceeds a critical value, the flow reaches sonic velocity and becomes independent of downstream pressure.

The power produced by the turbine is calculated using equation (12), which includes the beta correction factor to account for the additional work available from pulse energy. Turbine power output with pulse correction

$$P_t = \beta \times \dot{m}_t \times c_p, g \times T_t, in \times \left[1 - \left(\frac{P_t, out}{P_t, in}\right)^{\frac{\gamma_g - 1}{\gamma_g}}\right] \times \eta_t \qquad (12)$$

Where:

P_t= turbine power output (W)

β = beta correction factor for pulse flow (from Table 2.2)

$\dot{m}_t$= turbine mass flow rate (kg/s)

c_p, g = specific heat capacity of exhaust gas at constant pressure (J/kg·K)

T_t, in = turbine inlet gas temperature (K)

P_t, out= turbine outlet absolute pressure (Pa)

P_t, in= turbine inlet absolute pressure (Pa)

γ_g = ratio of specific heats for exhaust gas (approximately 1.33)

η_t= turbine isentropic efficiency (dimensionless)

The beta factor in equation (12) is greater than 1.0 for pulse turbocharging systems, meaning the turbine extracts more work from the pulsating flow than it would from steady flow at the same mean pressure. As

ISSN No. 2454-6194 | DOI: 10.51584/IJRIAS |Volume XI Issue VII July 2026

shown in Table 2.2, beta increases at lower engine loads where the pulse energy is stronger relative to the mean pressure.

The temperature of exhaust gas leaving the turbine is given by equation (13).Turbine outlet gas temperature

$$T_{out}, t = T_t, in - \eta_t \times T_t, in \times \left[1 - \left(\frac{P_t, out}{P_t, in}\right)^{\frac{\gamma g - 1}{\gamma g}}\right] \tag{13}$$

Where:

T_{out}, t = gas temperature at turbine outlet (K)

T_t, in = turbine inlet gas temperature (K)

η_t= turbine isentropic efficiency

P_t, out= turbine outlet pressure (Pa)

P_t, in = turbine inlet pressure (Pa)

γ_g= ratio of specific heats for exhaust gas

For proper turbocharger operation, the power produced by the turbine must equal the power consumed by the compressor, neglecting small mechanical losses in the turbocharger bearing. This matching condition is shown in equation (14). Turbocharger power balance

$$P_t = P_c + P_{tc}, loss \tag{14}$$

Where:

P_t= turbine power output (W)

P_c= compressor power consumption (W)

$P_{tc}, loss$= mechanical losses in turbocharger bearings (W)

For this study, the mechanical losses was assumed to be small (approximately 2 percent of turbine power) based on manufacturer data for modern turbochargers. This shows a good estimation of turbocharger speed, indicating proper power balance in the calibrated MVEM.

2.3.4 Exhaust Pulse Correction Factor Relationships

The alpha and beta correction factors introduced in equations (11) and (12) are related to the pulse factor, which characterises the strength of pressure pulsations in the exhaust system. Equation (15) defines the pulse factor. Pulse factor definition

$$\varphi = \frac{(P_{\max} - p_{min})}{P_{mean}} \tag{15}$$

where:

φ = pulse factor (dimensionless)

$P_{\max}$ = maximum pressure in the exhaust pulse (Pa)

p_{min}= minimum pressure in the exhaust pulse (Pa)

ISSN No. 2454-6194 | DOI: 10.51584/IJRIAS |Volume XI Issue VII July 2026

P_{mean}= mean pressure in the exhaust system (Pa)

A higher pulse factor indicates stronger pressure fluctuations. As shown in Table 2, the pulse factor increases from approximately 1.08 at full load to 1.23 at low load, indicating that pulsations are more significant at part load operation.

The relationship between the alpha correction factor and the pulse factor follows a decreasing trend as shown in equation (16).

Alpha factor as function of pulse factor

$$\alpha = 1 - k_1 \times \varphi \qquad (16)$$

Where:

α = alpha correction factor (dimensionless)

k_1 = empirical constant (approximately 0.12)

φ = pulse factor (dimensionless)

The alpha factor decreases as pulse factor increases because stronger pulsations cause more flow variation and reduce the effective mean flow through the turbine nozzle.

The beta correction factor increases with pulse factor as shown in equation (17). Beta factor as function of pulse factor

$$\beta = 1 + k_2 \times \varphi \qquad (17)$$

Where:

β = beta correction factor (dimensionless)

k_2 = empirical constant (approximately 0.15)

φ = pulse factor (dimensionless)

Equations (16) and (17) was used in the simulation to calculate alpha and beta at operating points where measured pulse data is not available, using the pulse factor derived from the exhaust receiver pressure.

The effective turbine flow area, when corrected for pulse effects, is given by equation (18). Effective turbine flow area with pulse correction

$$A_t, eff = \alpha \times A_t \qquad (18)$$

Where:

A_t, eff = effective turbine flow area (m²)

α = alpha correction factor

A_t= geometric turbine flow area (m²)

Similarly, the effective turbine work extraction is enhanced by the beta factor as shown in equation (19). Effective turbine work with pulse enhancement

$$W_t, eff = \beta \times W_t, steady \qquad (19)$$

here:

W_t, eff = effective turbine work per unit mass flow (J/kg)

β = beta correction factor

$W_t, steady$ = turbine work per unit mass flow under steady flow conditions (J/kg)

2.3.5 Engine Performance Parameters Under Back Pressure

The presence of static back pressure at the turbine outlet changes several engine performance parameters. The pumping work required to push exhaust gases out of the cylinders increases with back pressure. Equation (20) shows the additional pumping power required. Additional pumping power due to back pressure

$$P_{pump} = \dot{m}_{exh} \times \frac{(P_{back} - P_{amb})}{\rho_{exh}} \qquad (20)$$

Where:

P_{pump}= additional pumping power from back pressure (W)

$\dot{m}_{exh}$ = exhaust gas mass flow rate (kg/s)

P_{back} = static back pressure applied at turbine outlet (Pa)

P_{amb}= ambient pressure (Pa)

ρ_{exh} = density of exhaust gas at turbine outlet conditions (kg/m³)

The additional pumping power from equation (20) is supplied by the engine cylinders, which means either fuel consumption increases or brake power decreases unless the governor compensates by injecting more fuel. The exhaust gas temperature at the turbine inlet is affected by back pressure. Equation (21) gives this relationship based on engine operating conditions. Turbine inlet temperature under back pressure

$$T_t, in, BP = T_t, in, 0 + \frac{P_{pump}}{(\dot{m}_{exh} \times c_p, g)} \qquad (21)$$

Where:

T_t, in, BP = turbine inlet temperature with back pressure applied (K)

$T_t, in, 0$ = turbine inlet temperature with zero back pressure (K)

P_{pump}= additional pumping power from back pressure (W)

$\dot{m}_{exh}$= exhaust gas mass flow rate (kg/s)

c_p, g= specific heat capacity of exhaust gas (J/kg·K)

Equation (21) shows that each kilowatt of additional pumping work causes the exhaust temperature to increase by an amount that depends on the exhaust flow rate. At low loads where exhaust flow is small, the temperature increase from a given back pressure is larger than at high loads. This matches the trend observed in Table 3 where the temperature rise from back pressure was more significant at 1000 rpm than at 2600 rpm.

The air-excess ratio is a critical indicator of combustion quality and smoke formation. When back pressure increases, the air flow to the engine typically decreases while fuel flow increases, causing the air-excess ratio to drop. Equation (22) calculates the air-excess ratio. Air-excess ratio (lambda)

$$\lambda = \frac{\dot{m}_{air}}{(\dot{m}_f \times AF_{st})} \qquad (22)$$

ISSN No. 2454-6194 | DOI: 10.51584/IJRIAS |Volume XI Issue VII July 2026

Where all symbols have the same meaning as in equation (3). When lambda falls below approximately 1.3 to 1.5 for a marine diesel engine, smoke begins to appear in the exhaust due to incomplete combustion.

The maximum acceptable back pressure for any engine speed can be determined by setting a limit on either exhaust temperature or air-excess ratio. Equation (23) expresses this limit condition. Back pressure limit condition

$$P_{back,\max} = \min(P_{back} where\ T_t, in\ \leq\ T_{limit}\ and\ \lambda\ \geq\ \lambda_{limit}) \tag{23}$$

Where:

$P_{back,\max}$ = maximum allowable static back pressure (Pa)

T_{limit} = maximum allowable turbine inlet temperature (K)

λ_{limit}= minimum allowable air-excess ratio for smoke-free operation

For this study, typical limit values are T_{limit} =650°C(923 K) for turbine inlet temperature to prevent thermal damage, and λ_{limit}=1.3 to avoid visible smoke based on guidelines from Anderson, Salo, Fridell, and Winnes (2021) states that both smoke and thermal overloading simulated by the MVEM can be used as indicators to define limits of acceptable back pressure at any engine speed.

2.3.6 Mean Value Engine Model Governing Equations

The complete Mean Value Engine Model combines all the previous equations into a set of ordinary differential equations that describe how the engine states change with time. Equation (2.24) shows the differential equation for inlet receiver pressure dynamics. Inlet receiver pressure dynamics

$$\frac{dP_{inlet}}{dt} = \left(R\ \times \frac{T_{inlet}}{V_{inlet}}\right) \times \left(\dot{m}_{comp} - \dot{m}_{cyl}\right) \tag{24}$$

Where:

P_{inlet}= inlet receiver pressure (Pa)

t = time (s)

R = specific gas constant for air (J/kg·K)

T_{inlet} = temperature in inlet receiver (K)

V_{inlet} = volume of inlet receiver (m³)

$\dot{m}_{comp}$ = air flow rate from compressor (kg/s)

$\dot{m}_{cyl}$= air flow rate into cylinders (kg/s)

Equation (24) shows that inlet receiver pressure increases when compressor flow exceeds cylinder flow and decreases when cylinder flow exceeds compressor flow. In steady state, these two flows become equal.

Equation (2.25) gives the differential equation for exhaust receiver pressure dynamics. Exhaust receiver pressure dynamics

$$\frac{dP_{exh}}{dt} = \left(R_g \times \frac{T_{exh}}{V_{exh}}\right) \times \left(\dot{m}_{cyl}, out\ -\ \dot{m}_t\right) \tag{25}$$

Where:

P_{exh} = exhaust receiver pressure (Pa)

R_g = specific gas constant for exhaust gas (J/kg·K)

ISSN No. 2454-6194 | DOI: 10.51584/IJRIAS |Volume XI Issue VII July 2026

T_{exh} = temperature in exhaust receiver (K)

V_{exh} = volume of exhaust receiver (m³)

$\dot{m}_{cyl}, out$ = exhaust mass flow rate from cylinders (kg/s)

$\dot{m}_t$ = exhaust mass flow rate through turbine (kg/s)

The differential equations (2.24) and (2.25) will be solved numerically by the simulation software using time steps of 0.01 seconds. The simulation will run until all state variables reach steady values where the derivatives become zero.

RESULTS AND DISCUSSIONS

The results presented in this section are those computed from the methodology as stated in the previous chapter.

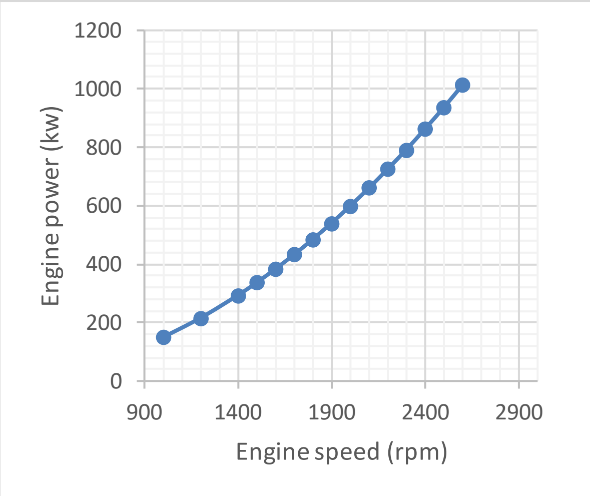

Figure 4: Measurement set-points along the propeller curve.

The Figure above shows the relationship between engine power (kw) and engine speed (rpm), also highlighting the 15 different set points. Figure. 4 shows that engine power, P, is directly proportional to the cube of the engine speed, n.

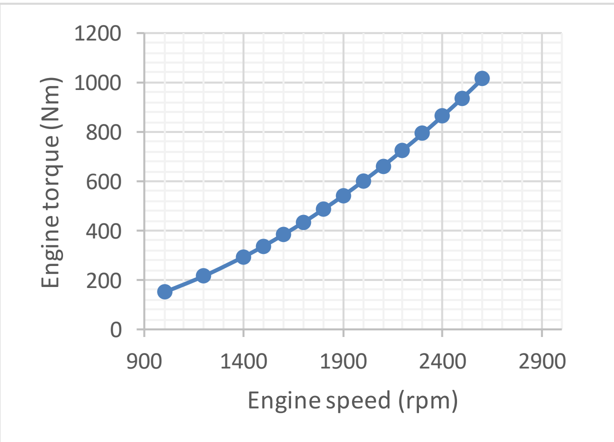

Figure 5: Engine torque vs engine speed curve

For the purpose of experiments, engine parameters were first measured at 15 different set-points (of load and engine speed), against three cases of back pressure. Figures. 4 and 5 depicts the 15 set points measured. In the first case, engine performance with no externally applied back pressure was measured. The second and the

ISSN No. 2454-6194 | DOI: 10.51584/IJRIAS |Volume XI Issue VII July 2026

third cases were for 0.25 mWC and 0.5 mWC of externally applied back pressure, respectively. For each case of back pressure, and at each set point, engine parameters such as temperature, pressure, air flow-rate and fuel consumption were measured. Expressing the engine speed and engine power in (%) of rated speed and power, we tabulate;

Table 4: Expressing the engine speed and engine power in (%) of rated speed and power.

Engine speed (rpm)		**Engine power (Kw)**	
RPM	RPM (%)	Load	Load (%)
2600	100	276	100
2500	96..2	245.4	88.9
2400	92.3	217.1	78.7
2300	88.5	191.1	69.2
2200	84.6	167.2	60.6
2100	80.8	145.4	52.7
2000	76.9	125.6	45.5
1900	73.1	107.7	39
1800	69.2	91.6	33.2
1700	65.4	77.2	28
1600	61.5	64.3	23.3
1500	57.7	53	19.2
1400	53.9	43.1	15.6
1200	46.2	27.1	9.8
1000	38.5	15.7	5.7

DETERMINATION OF CORRECTION FACTORS

Table 5: Values of α and β calculated from the discretization pulse

RPM %	**Load %**	**Factor values (using measured values)**	
		A	**B**
100	100	0.98	1.06
96.2	88.9	0.98	1.065
92.3	78.7	0.976	1.07
88.5	69.2	0.97	1.08
84.6	60.6	0.965	1.082
80.8	52.7	0.963	1.085
76.9	45.5	0.961	1.09
73.1	39	0.96	1.1
69.2	33.2	0.975	1.08
65.4	28	0.97	1.09
61.5	23.3	0.963	1.15
57.7	19.2	0.965	1.17
53.9	15.6	0.966	1.175
46.2	9.8	0.963	1.18
38.5	5.7	0.96	1.185

Table 5 shows the values of α and β for the pulse system on the test bench engine. As expected, the values of α were found to be less than 1, while that of β were greater than 1. Thus, showing that for a pulse system the

ISSN No. 2454-6194 | DOI: 10.51584/IJRIAS |Volume XI Issue VII July 2026

effective flow is lower and the effective turbine work is higher than that of a constant pressure system with the same mean pressure (as that of pulse) at the turbine inlet. In this way, the measured pressure pulses were used to derive the values of α and β correction factors given by Zinner. These values were then compared with simulated values of α and β, which were calculated in the model as a function of pulse factor using Eq. (3) and (4), given by Zinner.

CALIBRATION OF THE MVEM

Using the above discussed parameters and method, the MVEM was calibrated and matched to simulate the performance of the test engine. A number of parameters were iteratively adjusted while comparing the simulation results with the test-bench measurements. In this section, simulated engine parameters have been compared with test-bench measurements to showcase the calibrated and matched MVEM simulating the performance of the test engine only for the case of no external back pressure.

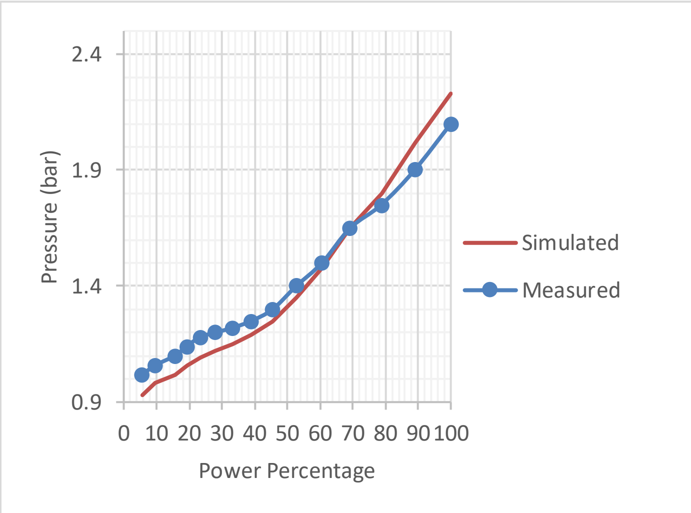

Figure 6: Comparison between measured and simulated inlet receiver pressure

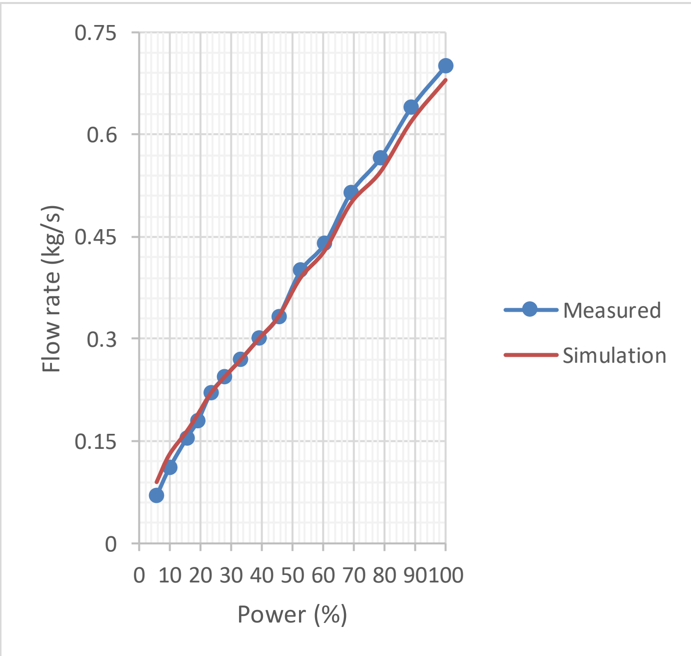

Figure 7: Comparison between measured and simulated inlet receiver pressure and air mass flow rate.

The first proof of a good match between simulation and measurements is visible from Figure. 6 and 7. These Figures present the compressor performance of the engine, obtaining the correct air flow for the corresponding pressure. For a good matching, it is also essential to simulate the temperatures as accurately as possible.

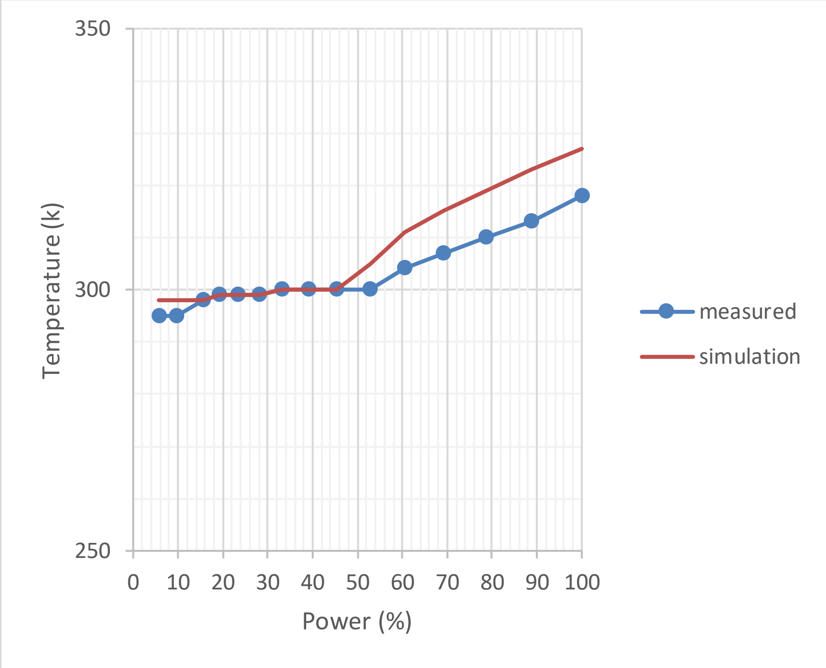

Figure 8: Comparison between measured and simulated inlet receiver temperature

Figure. 8 compares the simulated and measured inlet receiver temperature. The maximum error between the simulated and measured inlet receiver temperature is about 5 percent at 100 percent load.

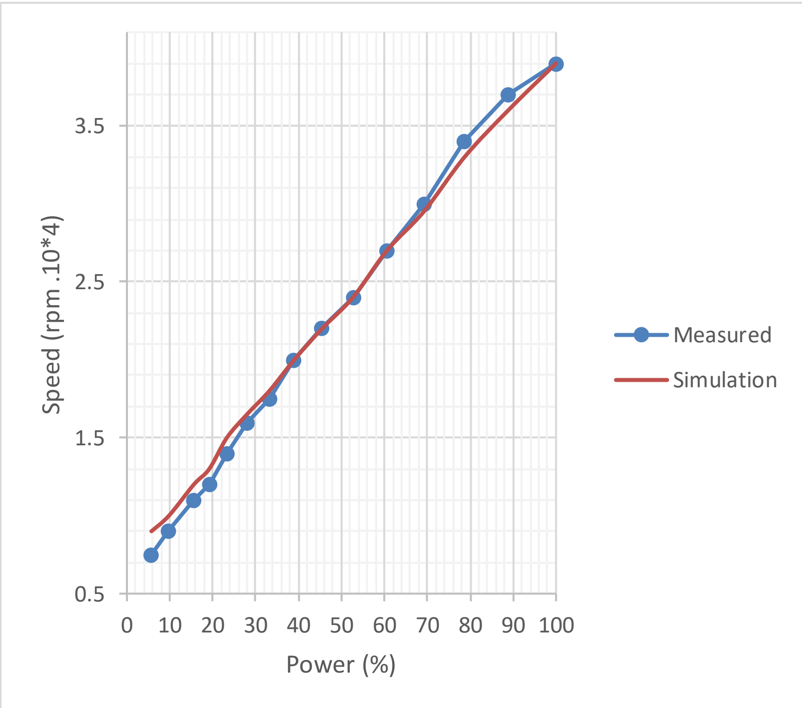

Figure 9: Comparison between measured and simulated turbocharger speed.

Furthermore, Figure. 9 shows a good estimation of turbocharger speed. The objective of a turbocharger model is to estimate the correct charge pressure and flow. However, it is also vital to estimate correct turbine pressures and temperatures. As explained earlier, the MVEM was applied to simulate the performance of a pulse turbocharged engine, which is not a mean value system and corrections had to be applied to the model. This gives deviations between simulated and measured turbine performance parameters. On the other hand, a constant pressure system (currently used turbocharger technology) would have a constant pressure in the outlet receiver, before the turbine, making it easier to simulate for a mean value model like the MVEM. Thus, the model would perform better with a constant pressure turbocharger system.

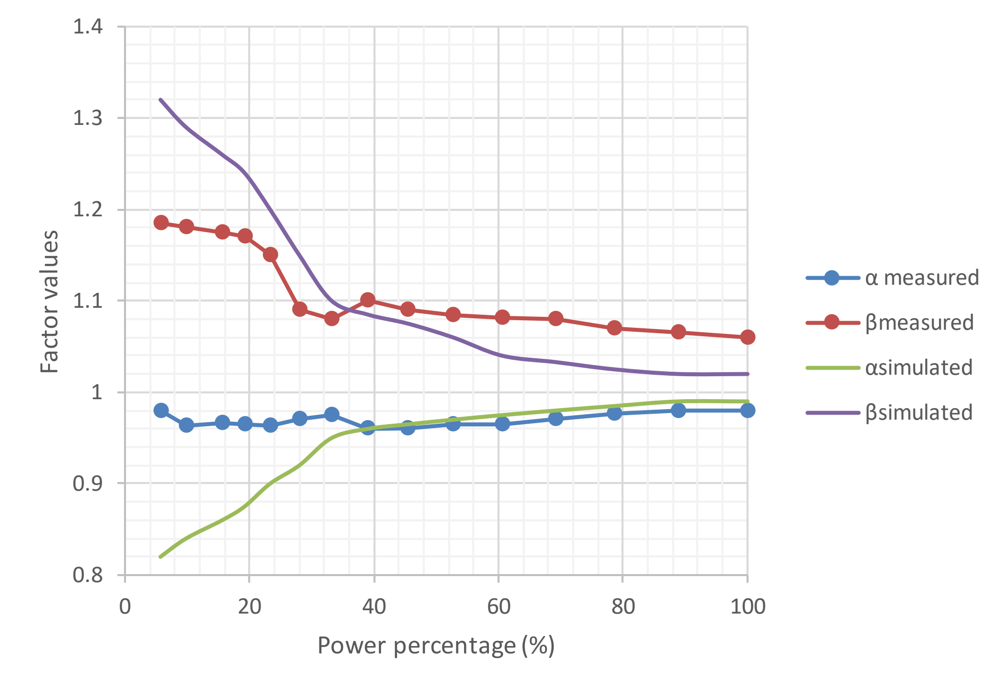

Figure 10: Comparison between α, β values obtained from simulation (s) and values calculated from measurements (m).

Focusing back to the validation, Figure. 10 shows the comparison between the values of α and β, simulated and the correction factors calculated for the measured turbine pulses, shown in Table 4.2.

As seen in Figure. 10, the b factor increases at part loads (or engine speeds along the propeller curve), implying an increase in work delivered by the turbine to the compressor. This is because at part loads the pulse factor increases, which increases the β value and decreases α. The increase in turbine work at part load is followed by an increase in the charge pressure and, hence, air flow rate, compared to the modern constant pressure systems. At the same time, the flow through the turbine drops, as the α factor drops with decreasing load. This is in alignment with the working principle of a pulse turbocharging system, which is known to improve part load performance of diesel engines by increasing the incoming flow-rate of air (Codan et al. 2005).

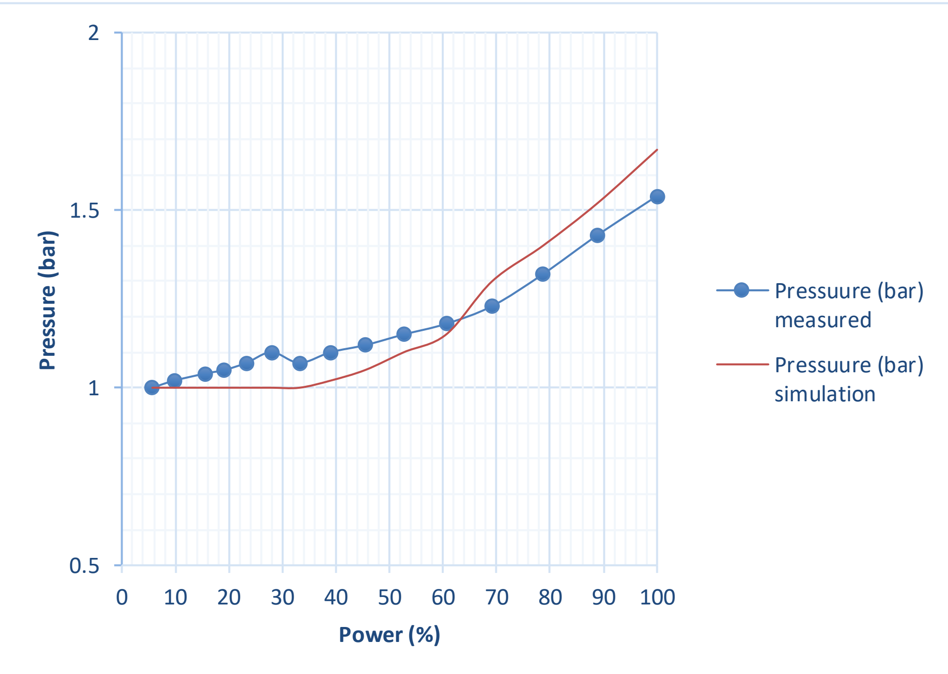

Figure. 11: Comparison between measured and simulated values for turbine inlet pressure.

However, as the MVEM is a mean value model, the turbine inlet pressure can closely simulate any one single value on the pressure pulse. Thus, an iterative method was adopted, where the turbine inlet pressure was matched to either the maximum or the mean or the minimum pulse pressure, by changing a number of parameters in the turbocharger model. The criterion for this matching is to acquire the correct charge pressure and incoming air flow rate (Figures. 6 - 10) as well as turbine temperature estimations, within 15 percent deviation from the measurements. Following this method, it was found that the model gave best results, for the above criterion, when turbine inlet pressure was made to simulate the lowest pulse pressure. This can be seen in Figures. 4.8 and 4.9.

In Figure. 11, the turbine inlet pressure shows a maximum deviation of about 10 percent, while the increasing trend of the measurements is well depicted by the model simulation as well.

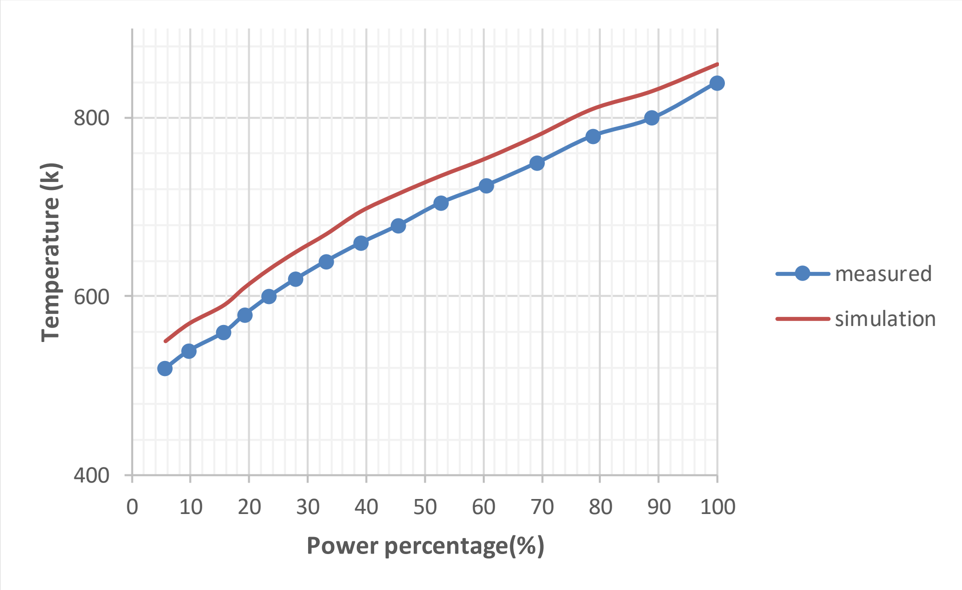

Figure. 12: Comparison between measured and simulated values for turbine inlet temperature

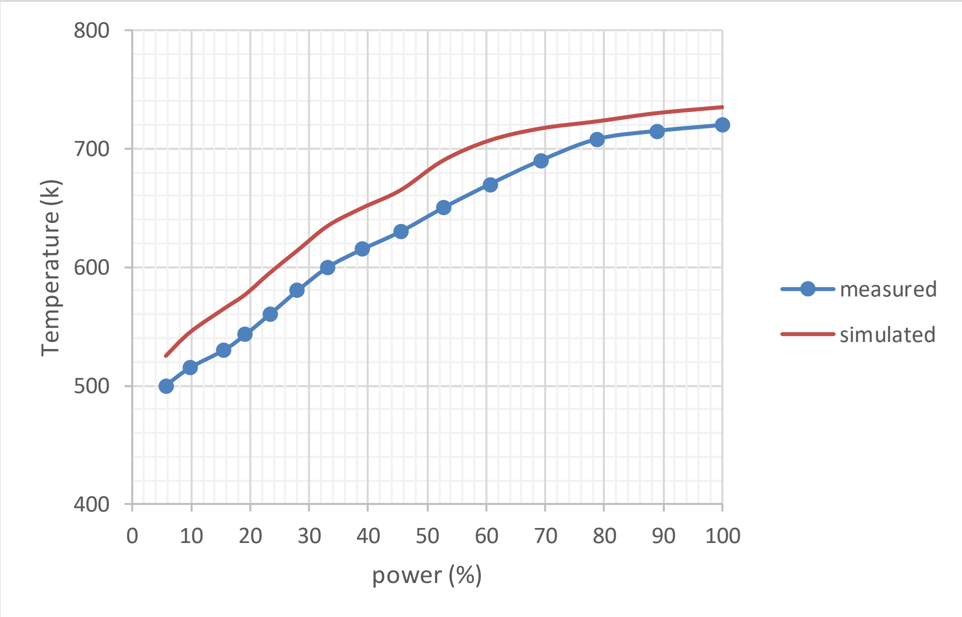

Figure. 13: Comparison between measured and simulated values for turbine outlet temperature

Besides this, the turbine inlet temperature gives a maximum percentage difference of about 9 percent, at lowest load, and a difference of about 12 percent for turbine outlet temperature, as seen in Figure. 12 and 13.

This concludes the calibration and matching of the MVEM to simulate the performance of the pulse turbocharged test engine.

This section also highlighted the shortcomings of the model related to the difficulty in simulating the pressure pulse. However, in a separate study this mode successfully simulated the performance of an engine running with a constant pressure turbocharger system (Sapra, 2015).

Validation of MVEM: effects of back pressure on engine performance

In this section, the calibrated and matched model is validated against measurement with external back pressure.

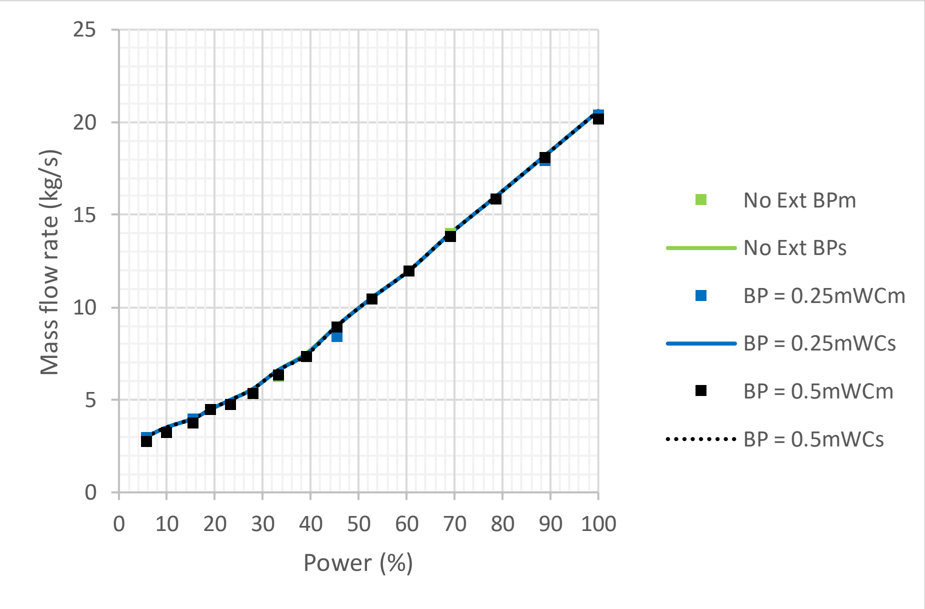

Figure. 14: Back pressure effect on fuel consumption based on measurements (m) and simulations (s).

Increased back pressure means the engine would need to do more work to pump out the exhaust gases. However, the load demand from the water-brake remains constant. This decelerates the engine, activating the governor, which pushes in more fuel in order to offset the deceleration. Thus, an increase in back pressure would increase the fuel consumption. Simulations and measurements exhibited a small increase in fuel consumption of about 3 percent at 42 percent load and 0.5 mWC of back pressure. Figure. 14 shows the minor increase in fuel consumption due to increased back pressure.

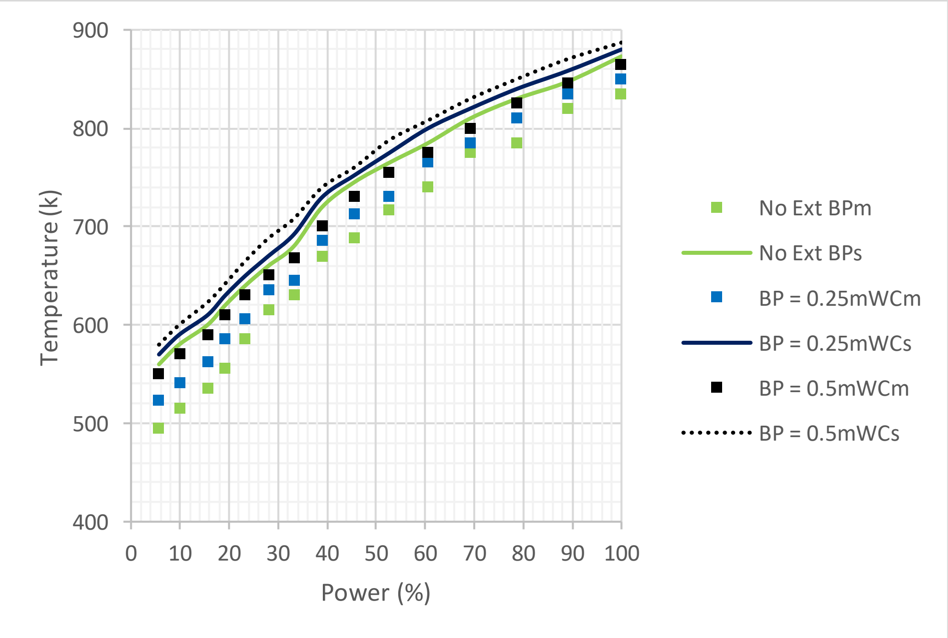

Figure. 15: Back pressure effect on turbine inlet temperature based on measurements (m) and simulations(s).

ISSN No. 2454-6194 | DOI: 10.51584/IJRIAS |Volume XI Issue VII July 2026

Therefore, back pressure causes an increase in fuel consumption (even though small) and drops air intake, leading to incomplete combustion and increase in in-cylinder and exhaust receiver temperatures, as seen in Figure. 15. Measurements and simulations show that the rise in turbine inlet (exhaust receiver) temperature due to back pressure is more significant at lower loads than at higher loads. Based on measurements, turbine inlet temperature increased by a maximum of 6.7 percent at lowest load; and by 4.5 percent based on simulations. Thus, the relative increase in temperatures predicted by simulations matched the measured.

Excessive exhaust gad (exhaust receiver) temperatures can increase thermal stresses and cause serious damage to the turbocharger. Excessive exhaust temperatures can damage seals and grooves causing unintended oil and exhaust gas leakage (Idzior, not dated). High exhaust gas temperatures can also lead to a coked centre housing, which will affect turbocharger performance and life.

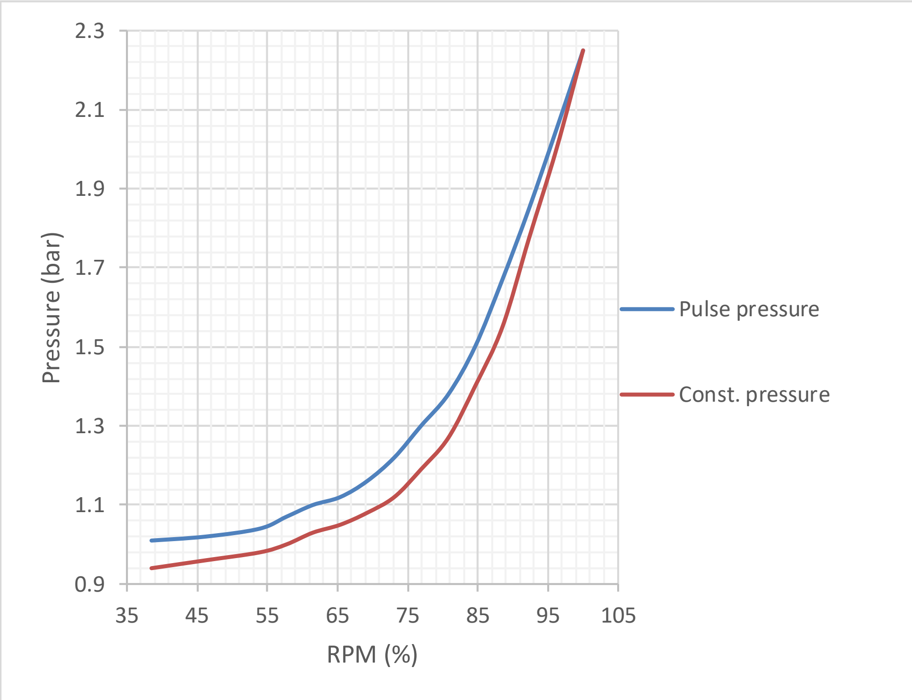

Figure. 16: Comparison between inlet receiver pressure delivered by a pulse turbocharger and constant pressure turbocharger, with a 30 degree valve overlap engine

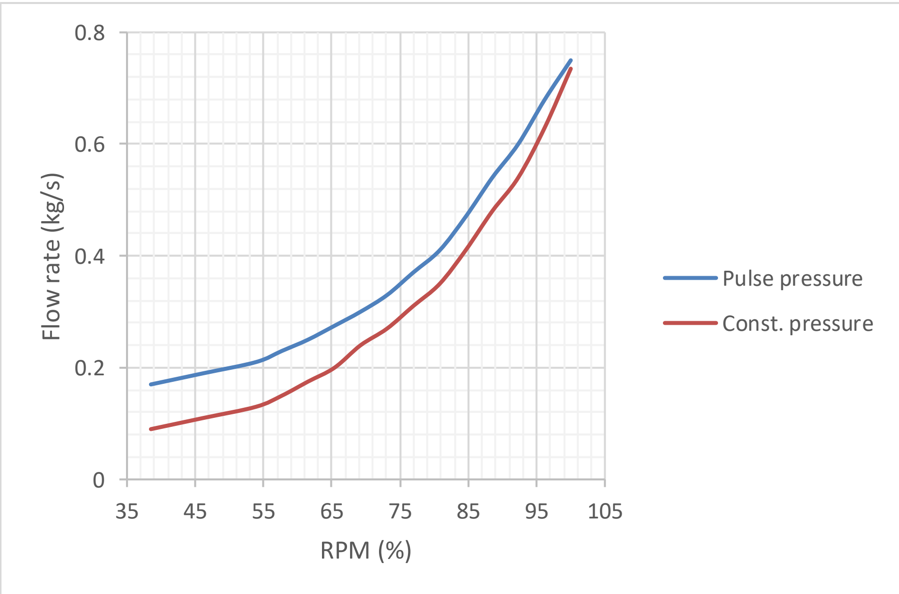

Figure 17: Comparison between air mass-flow rate delivered by a pulse turbocharger and constant pressure turbocharger, with a 30 degree valve overlap engine

Figures. 15 and 17 shows that at rated speed the pulse turbocharger and constant pressure turbocharger have almost equal values of inlet receiver pressure and air flow rate. However, at lower rpms (or load along the propeller curve) the pulse system delivers much higher values of charger pressure and air intake compared to the constant pressure turbocharger. Simulations show that the air intake for a pulse turbocharger is more by about 68 percent, at lowest speed, when compared to that delivered by a constant pressure system. This drastically improves the back pressure handling capabilities of the engine as depicted in Figures. 18 and 19 compared to a constant pressure turbocharger system and large valve overlap.

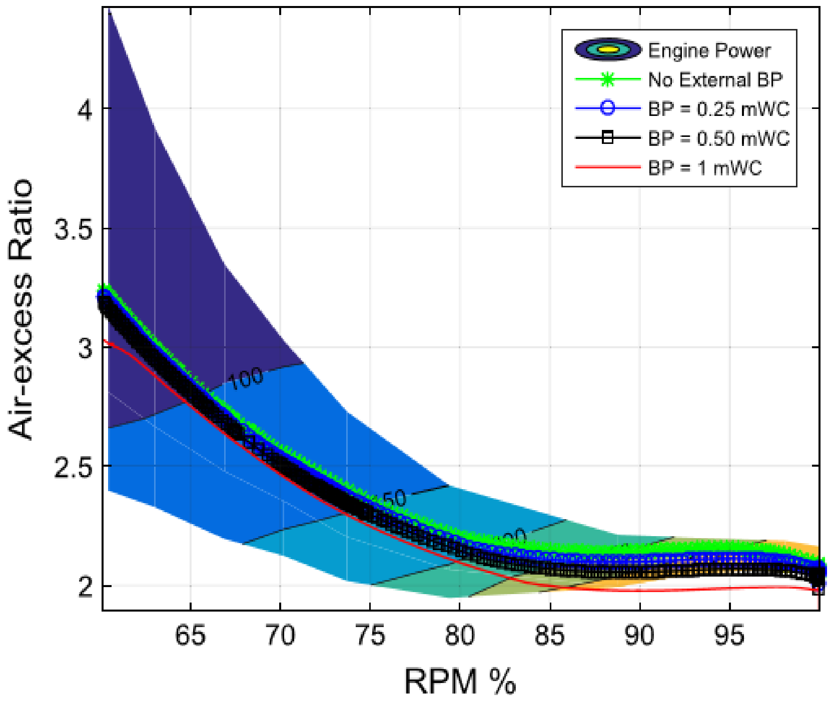

Figure. 18: Back pressure effect on air-excess ratio of a constant pressure turbocharged engine, with 30 degree valve overlap.

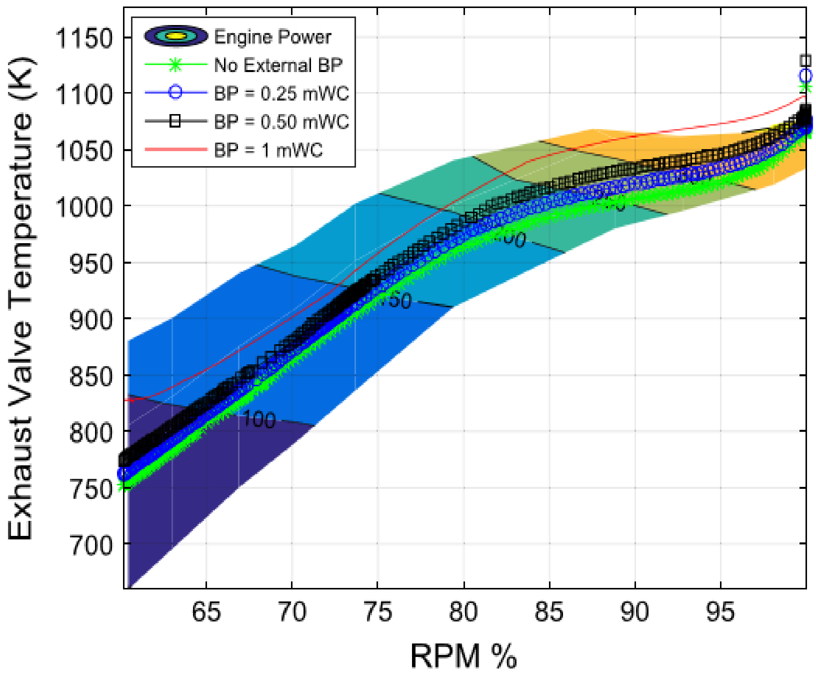

Figure. 19: Back pressure effect on exhaust valve temperature of a constant pressure turbocharged engine, with 30 degree valve overlap.

As evident in Figures. 4.15 and 4.16, the 30 degree valve overlap engine with a pulse turbocharger can sustain 1 mWC of back pressure with signs of thermal overloading only above 90 percent engine speed. Furthermore, Figures. 4.15 and 4.16 shows that the air-excess ratio of a pulse turbocharged engine hardly drops below about 1.9 at a back pressure of 1 mWC, indicating no signs of engine smoke. The model shows that such a system would easily be able to counter the high values of back pressure due to the pulse effect, and also reduced back flow in case of any negative scavenging (smaller valve overlap). This would cancel the need to switch to an above water exhaust, at lower rpms.

This section shows that both smoke and thermal overloading, simulated by the MVEM, can be used as an indicator to define limits of acceptable back pressure at any engine speed. A thermally overloaded engine can be unloaded by either reducing engine power or back pressure.

This section also proves that a pulse turbocharged engine and a small overlap can drastically help improve back pressure handling capabilities of an engine compared to a constant pressure turbocharger system and large valve overlap.

CONCLUSIONS

This work investigated how static back pressure affects a marine diesel engine by combining experimental measurements with simulation modelling using a Mean Value Engine Model. The experiments showed that applying back pressure raises exhaust gas temperatures and increases fuel consumption, with temperature rises being more noticeable at low engine loads than at high loads. The simulation model, after calibration with measured correction factors alpha and beta for the pulse turbocharging system, predicted engine behaviour with good accuracy, keeping most errors below ten to twelve percent when compared to test measurements. The findings confirm that a pulse turbocharged engine delivers higher air flow and charge pressure at low speeds than a constant pressure system, which helps the engine handle back pressure better. The model also demonstrated that the air-excess ratio stays above 1.9 even at one metre of water column back pressure, indicating no risk of visible smoke, while thermal overloading appears only above ninety percent engine speed. Therefore, the validated simulation tool can be used to set safe back pressure limits for engine operation, and the results prove that pulse turbocharging with small valve overlap greatly improves an engine's ability to withstand exhaust restrictions without major losses in performance or efficiency.

REFERENCES

1. Sardar, A Islam, R., Anantharaman, M. & Garaniya, V. (2025). Advancements and obstacles in improving the energy efficiency of maritime vessels: A systematic review,Marine Pollution Bulletin,Volume 214,
2. Sheng Liu, Ling Leng, Wenjie Zhou, Lei Shi, (2021).Optimizing the Exhaust System of Marine Diesel Engines to Improve Low-speed Performances and Cylinder Working Conditions,Fluid Dynamics and Materials Processing,Volume 17, Issue 4,Pages 683-695,
3. Auto Exhaust Guide. (n.d.). *The role of backpressure in exhaust system tuning and performance enhancement*. Retrieved June 16, 2026, from https://autoexhaustguide.com/article/the-role-of-backpressure-in-exhaust-system-tuning-and-performance-enhancement/
4. Zannis, T. C., Katsanis, J. S., Christopoulos, G. P., Yfantis, E. A., Papagiannakis, R. G., Pariotis, E. G., Rakopoulos, D. C., Rakopoulos, C. D., & Vallis, A. G. (2022). Marine Exhaust Gas Treatment Systems for Compliance with the IMO 2020 Global Sulfur Cap and Tier III NO_x Limits: A Review. *Energies*, *15*(10), 3638.
5. Zincir,B.A.(2025).Transitioning to sustainable shipping: A multidimensional analysis of maritime emission strategies,Ocean & Coastal Management,Volume 269,
6. Khanyi, N., Inambao, F., & Stopforth, R. (2025). Prediction of Diesel Engine Performance and Emissions Under Variations in Backpressure, Load, and Compression Ratio Using an Artificial Neural Network. *Applied Sciences*, *15*(19), 10588

ISSN No. 2454-6194 | DOI: 10.51584/IJRIAS |Volume XI Issue VII July 2026

7. Xin, R., Zhai, J., Liao, C., Wang, Z., Zhang, J., Bazari, Z., & Ji, Y. (2022). Simulation Study on the Performance and Emission Parameters of a Marine Diesel Engine. *Journal of Marine Science and Engineering*, *10*(7), 985.
8. Ceylan, B.O., Karatuğ, Ç. & Arslanoğlu, Y. (2022). A novel methodology for the use of engine simulators as a tool in academic studies. *Journal of Marine Science and Technology*27, 1220–1232.
9. Huang, L., Liu, J., Liu, R., Wang, Y., & Liu, L. (2022). Experimental Investigation on Combustion and Performance of Diesel Engine under High Exhaust Back Pressure. *Machines*, *10*(10), 919.
10. Hilgers, M. (2022). The Exhaust System. In: The Diesel Engine. Commercial Vehicle Technology. Springer Vieweg, Berlin, Heidelberg.
11. Nwoka, B. G., Chuku, A. J. & Ekine, A. A. (2026). Numerical assessment of marine coating materials, balancing, performance and environmental compatibility. Global Journal of Engineering and Technology Advances, 26(03), 168-180.
12. Leyira, N. A., Kombo, T.-J., & Samson, N. (2026). Reliability assessment of predictive maintenance techniques for marine propulsion systems. *Irish International Journal of Engineering and Applied Sciences, 10*(2), 27–51.
13. Oludi, K., & Nwoka, B. G. (2025). Hydrodynamic analysis and environmental adaptation of a trimaran model for Nigerian coastal and inland waters. *Journal of Newviews in Engineering and Technology*, *7*(1), 119–130.